Available online at www.sciencedirect.com
SCIENCE DIRECT®
Journal of Organometallic Chemistry 689 (2004) 4407–4419
Journal of Organometallic Chemistry
www.elsevier.com/locate/jorganchem

Structural investigations on new iron-acyl derivatives of $B(C_6F_5)_3$

Grant D.W. Anderson, Oliver J. Boys, Andrew R. Cowley, Jennifer C. Green *, Malcolm L.H. Green *, Simon A. Llewellyn, Carlo Maresca von Beckh, Sofia I. Pascu [1], Ino C. Vei

Inorganic Chemistry Laboratory, South Parks Road, Oxford OX1 3QR, UK

Received 15 June 2004; accepted 5 July 2004
Available online 6 August 2004

Abstract

Reactions between $[Fe(\eta\text{-}C_5H_5)(MeCO)(CO)(L)]$, L = PPh_3 (**1**), PMe_3 (**2**), $PPhMe_2$ (**3**), PCy_3 (**4**), CO (**5**), and $B(C_6F_5)_3$ give new complexes $[Fe(\eta\text{-}C_5H_5)\{MeCOB(C_6F_5)_3\}(CO)(L)]$ L = PPh_3 (**7**), PMe_3 (**8**), $PPhMe_2$ (**9**), PCy_3 (**10**), CO (**11**), where $B(C_6F_5)_3$ coordinates selectively to the O-acyl groups. Hydrolysis of **7** gives $[Fe(\eta\text{-}C_5H_5)\{HOB(C_6F_5)_3\}(CO)(PPh_3)]$ (**6**). The X-ray structures of **6**, **8** and **11** have been determined. Calculations, using density functional theory, demonstrate that the charge transfer to the acyl group on Lewis acid coordination is more significant in the σ than the π system. Both effects lead to a lengthening of the acyl C–O bond thus π populations cannot be inferred from the distance changes.

Keywords: Fischer–Tropsch reactions; Tris(perfluorophenyl)borane; Lewis acids; Catalysis; Fe-acyls complexes; Fischer carbenes; Density functional theory

1. Introduction

The transition metal catalysed reductive polymerisation of carbon monoxide by dihydrogen to form hydrocarbons, the Fischer–Tropsch (FT) synthesis, has received renewed interest in recent years [1]. However, the search for a homogenous Fischer–Tropsch catalyst has been unfruitful. A possible model for a homogeneous FT catalyst could be found in two centre/bridging systems such as M–CO → Z, where Z is an electron-poor and oxophilic metal or a Lewis acid [2] (Scheme 1). Here, the metal centre M is proposed to act as a support for chain growth, while Z activates the M-acyl functionality towards hydrogenation. Successive carbonylation and reduction could then lead to carbon chain homologation.

The $[Fe(\eta\text{-}C_5H_5)(CO)_2]$ moiety and its congeners, in which $(\eta\text{-}C_5(CH_3)_5)$ or (η-indenyl) replace $(\eta\text{-}C_5H_5)$, have been extensively investigated [3,4]. In particular, a large body of research has centred on the use of such systems as chiral auxillaries [5–7]. However, catalytic hydrogenation of metal–carbonyl ligands such as M–CO, M–CHO, M–COR has not been established. The reduction of the metal-coordinated CO in the compounds $[M(\eta\text{-}C_5H_5)(CO)_3(PPh_3)]^+$ (M = Mo, W) with $NaBH_4$ gives the methyl complexes $[M(\eta\text{-}C_5H_5)(CH_3)(CO)_2(PPh_3)]$ [8]. The strong reducing agent BH_3THF has also been used for the reduction of metal-acyl groups [9]. The reduction by lithium aluminium hydride of a terminal CO group in $[Fe(\eta\text{-}C_5(CH_3)_5)(PMe_3)(CO)_2]^+$ gives $[Fe(\eta\text{-}C_5(CH_3)_5)(PMe_3)(CO)(CH_3)]$ [10]. Akita et al. [11] have shown that the reaction of the acetyl compound $[Fe(\eta\text{-}C_5H_5)(MeCO)(CO)(PPh_3)]$ with H_2SiPh_2 and the catalyst

* Corresponding authors. Tel.: +44-1865-272637; fax: +44-1865-272690.
E-mail address: jennifer.green@chem.ox.ac.uk (J.C. Green).
[1] Present address: Department of Chemistry, University of Cambridge, Lensfield Road, CB4 1EW.

0022-328X/$ - see front matter © 2004 Elsevier B.V. All rights reserved.
doi:10.1016/j.jorganchem.2004.07.013

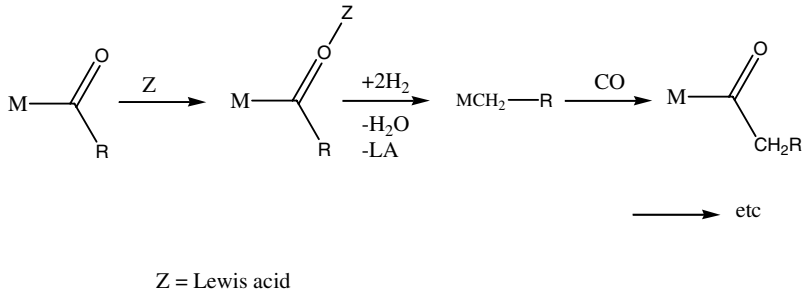

Scheme 1. A possible mechanism for homogeneous FT reactions.

$[RhCl(PPh_3)_3]$ gives $[Fe(\eta\text{-}C_5H_5)(Et)(CO)(PPh_3)]$. Subsequent treatment with CO and $[Fe(\eta\text{-}C_5H_5)_2][BF_4]$ gives $[Fe(\eta\text{-}C_5H_5)(EtCO)(CO)(PPh_3)]$. This sequence of reduction and insertion can be repeated to give the pentanoyl complex $[Fe(\eta\text{-}C_5H_5)(COC_4H_9\})(CO)(PPh_3)]$. Treatment of $[Fe(\eta\text{-}C_5H_5)(MeCO)(CO)(PPh_3)]$ with HBF_4 or $R_3O^+BF_4^-$, (where R = Me, Et), results in selective attack at the acyl-O atom giving $[Fe(\eta\text{-}C_5H_5)(MeCOR)(CO)(PPh_3)][BF_4]$ [12]. Davies et al. have demonstrated that treatment of $[Fe(\eta\text{-}C_5H_5)(CO)(PPh_3)(COEt)$ with trimethyloxonium tetrafluoroborate led to the formation of $[Fe(\eta\text{-}C_5H_5)$

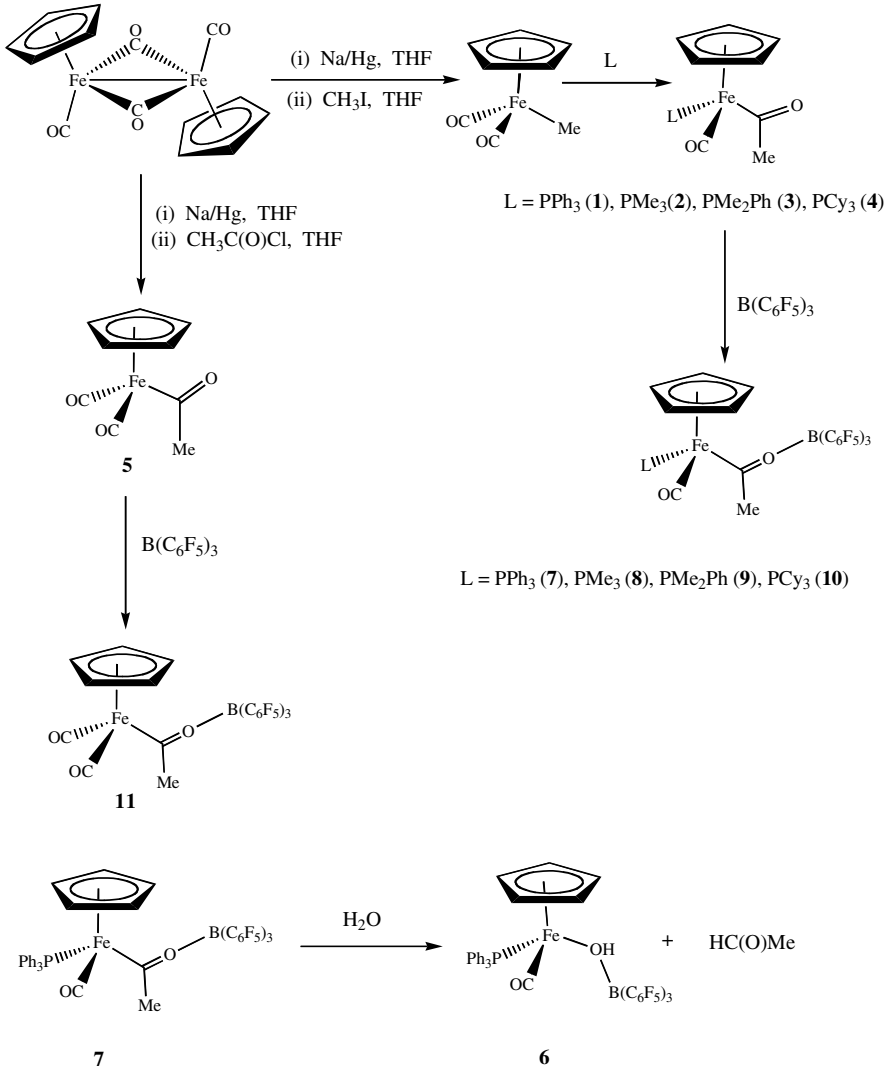

Scheme 2. Formation of compounds **1–5** and **7–11**.

$(CO)(PPh_3)(=COMe)Et]^+$, which underwent reduction on treatment with hydride reagents to give $[Fe(\eta\text{-}C_5H_5)(CO)(PPh_3)(CH(OMe)Et)]$ [13]. $[Fe(\eta\text{-}C_5H_5)(CO)CH_3)(CO)_2]$ has been shown to react with BF_3 gives the acetyl O-coordinated adduct $[Fe(\eta\text{-}C_5H_5)(CO\{BF_3\}CH_3)(CO)_2]$ [14].

Recently, $B(C_6F_5)_3$ (a strong Lewis acid) has been used as a catalyst for the hydrosilylation of aromatic and aliphatic carbonyls [15]. Unlike BF_3, the pentafluorophenyls of $B(C_6F_5)_3$ are not readily detached from the boron centre. Therefore, we set out to prepare and study $B(C_6F_5)_3$ adducts of the iron-acetyl complexes $[Fe(\eta\text{-}C_5H_5)(COCH_3)(CO)(L)]$ (where L = PPh_3 (**1**), PMe_3 (**2**), $PPhMe_2$ (**3**), PCy_3 (**4**), CO (**5**)). Studies using density functional theory (DFT) of several model compounds containing the systems [Fe-acyl] and [Fe-acyl-BF_3] provide insight into their electronic structure.

2. Results and discussion

2.1. Reactions

Scheme 2 shows synthetic routes used for the compounds **1–11**. The complexes $[Fe(\eta\text{-}C_5H_5)(MeCO)(CO)(L)]$, where L is PPh_3 (**1**), PMe_3 (**2**), $PPhMe_2$ (**3**), PCy_3 (**4**), and CO (**5**) have been described previously [12,16,17]. These compounds were synthesized using modifications of the reported routes and then reacted with $B(C_6F_5)_3$. It has been shown that $B(C_6F_5)_3$ reacts with $[Fe(\eta\text{-}C_5H_5)Me(CO)_2]$ [18] to give the unexpected complex $[Fe\text{-}s\text{-}C_6F_4(2\text{-}C(O)Me)](\eta\text{-}C_5H_5)(CO)]$. However, NMR scale reactions of $B(C_6F_5)$ in d^8-toluene with the compounds $[Fe(\eta\text{-}C_5H_5)(COCH_3)(CO)(L)]$, where L is a tertiary phosphine or CO, showed that only adducts of the type $[Fe(\eta\text{-}C_5H_5)\{MeCOB(C_6F_5)_3\}(CO)(L)]$ were formed. The larger scale reactions between complexes **1–5** and $B(C_6F_3)_3$ in toluene also led in all cases to formation of the acyl-$B(C_6F_5)_3$ adducts **7–11** in good yields. The complex $[Fe(\eta\text{-}C_5H_5)\{HOB(C_6F_5)_3\}(CO)(PPh_3)]$ (**6**) was formed as a result of the hydrolysis of **7**, when the product was purified by chromatography over silica. A proposed pathway for the formation of **6** is shown in Scheme 3. The adduct $[H_2OB(C_6F_5)_3]$ [19] is presumably formed initially. This strong acid would be expected to protonate the [Fe-acyl] group to form a Fischer-carbe ne-type intermediate [12]. Subsequent dissociation with elimination of HC(O)Me gives the observed $[Fe(\eta\text{-}C_5H_5)\{HOB(C_6F_5)_3\}(CO)(PPh_3)]$ (**6**).

2.2. Spectroscopic data

The IR spectra (in Nujol for **1–5** and **7–11** and in d^8-toluene for **6**), and the ^1H, $^{31}P\{^1H\}$, $^{11}B\{^1H\}$, and ^{19}F NMR spectra are given in Table 1. The IR spectra of compounds **1–11** all show sharp bands in the region characteristic for CO stretching frequencies. In all cases, the coordination of $B(C_6F_5)_3$ to the acyl oxygen results in a significant lowering of the carbonyl stretching frequency, which made them unobservable as Nujol emulsions. This is consistent with increased single-bond character of the acyl-C–O. There is a rise in the terminal carbonyl absorption of ca. 55 cm^{-1} as a consequence of the reduced electron density on the cationic iron centre of the $B(C_6F_5)_3$ adducts. The IR spectra of $[Fe(\eta\text{-}C_5H_5)\{MeCOB(C_6F_5)_3\}(CO)(PCy_3)]$ (**10**) and the other

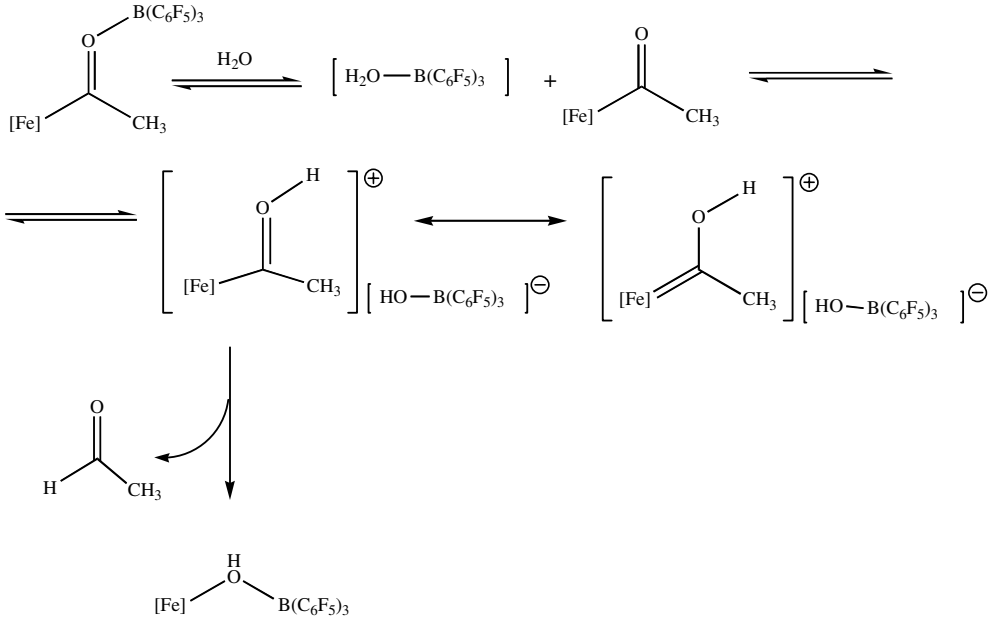

Scheme 3. Proposed pathway for the formation of **6**.

Table 1
IR (Nujol, ν in cm^{-1}) and NMR data (d^8-toluene unless otherwise specified, δ in ppm, J in Hz) at room temperature

Compound	IR (υ_{CO})		^1H	$^{31}P\{^1H\}$	$^{11}B\{^1H\}$	^{19}F-*ortho*	^{19}F-*meta*	^{19}F-*para*
	Terminal	Acyl						
$[Fe(\eta\text{-}C_5H_5)(MeCO)(CO)(PPh_3)]$[a] (**1**)	1902s	1600 m	2.60 (3H, s, CO*Me*) 4.28 (5H, d, $^3J_{PH}$ 1, *Cp*) 7.06 (9H, m, *m* + *p-Ph*) 7.74 (6H, m, *o-Ph*)	77.6				
$[Fe(\eta\text{-}C_5H_5)(MeCO)(CO)(PMe_3)]$[b] (**2**)	1914s	1604 m	1.22 (9H, d, $^2J_{PH}$ = 10, P*Me*$_3$) 2.41 (3H, s, CO*Me*) 4.35 (5H, b, *Cp*)	44.8				
$[Fe(\eta\text{-}C_5H_5)(MeCO)(CO)(PMe_2Ph)]$ (**3**)	1916s	1605 m	1.41 (6H, d, $^2J_{PH}$ 8.7, P*Me*$_3$) 2.48 f(3H, b, CO*Me*) 4.31 (5H, s, *Cp*) 7.32 (3H, s, *m* + *p-Ph*) 7.48 (2H, s, *o-Ph*)	52.0				
$[Fe(\eta\text{-}C_5H_5)(MeCO)(CO)(PCy_3)]$ (**4**)	1914s	1623 m	2.51 (33H, m, P*Cy*$_3$) 2.58 (3H, s, CO*Me*) 4.53 (5H, s, *Cp*)	75.3				
$[Fe(\eta\text{-}C_5H_5)(MeCO)(CO)_2]$ (**5**)	2023s 1966s	1666 m	2.37 (3H, s, CO*Me*) 4.68 (5H, s, *Cp*)	–				
$[Fe(\eta\text{-}C_5H_5)\{HOB(C_6F_{53})\}(CO)(PPh_3)]$[a] (**6**)	1973s	–	2.60 (1H,b, *H*O) 4.18 (5H, s, *Cp*) 7.00 (15H, m, *Ph*)	69.0	−0.68	−141.3 (b)	−165.5 (b)	−156.9 (b)
$[Fe(\eta\text{-}C_5H_5)\{MeCOB(C_6F_5)_3\}(CO)(PPh_3)]$ (**7**)	1957s	–	2.21 (3H, s, CO*Me*) 4.18 (5H, s, *Cp*) 7.00 (9H, s, *m* + *p-Ph*) 7.22 (6H, s, *o*-Ph)	78.66	−14.0	−132.9 (d, $^3J_{FF}$ 17)	−167.1 (td, $^3J_{FF}$ 21.1, $^4J_{FF}$ 5.6)	−160.9 (t, $^3J_{FF}$ 20.3)
$[Fe(\eta\text{-}C_5H_5)\{MeCOB(C_6F_5)_3\}(CO)(PMe_3)]$ (**8**)	1948s	–	0.81 (9H, d, $^2J_{PH}$ 7, P*Me*$_3$) 2.34 (3H, s, CO*Me*) 3.98 (5H, d, $^4J_{PH}$ 2, *Cp*)	43.1	−13.9	−133.2 (d, $^3J_{FF}$ 22.5)	−164.1 (td, $^3J_{FF}$ 22.5, $^4J_{FF}$ 11.3)	−157.5 (t, $^3J_{FF}$ 21.2)
$[Fe(\eta\text{-}C_5H_5)\{MeCOB(C_6F_5)_3\}(CO)(PMe_2Ph)]$ (**9**)	1952s	–	1.85 (6H, d, $^2J_{PH}$ 1, P*Me*$_2$) 2.09 (3H, s, CO*Me*) 3.73 (5H, s, *Cp*) 6.78 (3H, m, *m* + *p-Ph*) 6.88 (2H, m, *o-Ph*)	36.7	−19.2	−139.9 (d, $^3J_{FF}$ 21.3)	−172.5 (b)	−165.8 (t, $^3J_{FF}$ 20.2)

[Fe(η-C_5H_5){MeCOB(C_6F_5)$_3$}(CO)(PCy$_3$)] (**10**)	2048s, 2005s	–	1.52 (33H, m, P*Cy*$_3$) 2.72 (3H, s, CO*Me*) 4.23 (5H, s, *Cp*)	80.1	−14.1	−133.5 (d, $^3J_{FF}$ 22.6)	−170.0 (td, $^3J_{FF}$ 22.6)	−167.5 (b)	
[Fe(η-C_5H_5){MeCOB(C_6F_5)$_3$}(CO)$_2$] (**11**)	2052s	–	2.04 (3H, s, CO*Me*)	–	−1.5	−134.5 (d, $^3J_{FF}$ 20.9)	−163.8 (td, $^3J_{FF}$ 22.7, $^4J_{FF}$ 7.3)	−156.9 (t, $^3J_{FF}$ 20.5)	
	1994s		3.88 (5H, s, *Cp*)						
B(C_6F_5)$_3$	–	–	–	–	58	−128.8(b)	−144.6(b)	−161.5(b)	

ν_{OH} 3229 cm^{-1}.
[a] C_6D_6.
[b] $CHCl_3$.

related adducts with bulky tertiary phosphine ligands show two bands in the C–O stretching region indicating two distinct terminal carbonyl stretches. These are assigned to the presence of conformational isomers [20].

The complex **6**, shows a broadband at 3229 cm^{-1} that may be assigned to the H–O stretching vibration of [HOB(C_6F_5)$_3$]. The terminal CO absorption, lies at a higher wave number than for the neutral parent [Fe(η-C_5H_5)($COCH_3$)(CO)(PPh_3)], as is expected for a weakly bonded [HOB(C_6F_5)$_3$]$^-$ adduct. Facile separation into the ion pair [Fe(η-C_5H_5)(CO)(PPh_3)]$^+$[HOB(C_6F_5)$_3$]$^-$ may occur in solution.

The ^{1}H NMR spectra of **7**–**11** show a decrease of the chemical shift of CO*Me* upon coordination of B(C_6F_5)$_3$ to the acyl-oxygen. In all cases, the C_5H_5-resonances are found up-field compared with the parent compounds, the most shielded being **7** and **9**. The increase may be caused the electron withdrawing effect of B(C_6F_5)$_3$. The ^{19}F NMR spectra of **7**–**11**, show an upfield shift in the *para*-fluorine (ca. 12 ppm) compared to uncoordinated B(C_6F_5)$_3$. The ^{11}B NMR spectra are particularly diagnostic since the ^{11}B resonances differ substantially between the three-coordinate borane and the four-coordinate boron in the Lewis acid–base adducts. The latter resonances are shifted up-field with respect to B(C_6F_5)$_3$ by ca. 50 ppm [19,21–23].

2.3. X-ray crystallography

Table 2 contains selected molecular parameters. A summary of the X-ray crystallographic data for compounds **6**, **8** and **11** is given in Table 3. The ORTEP diagrams are presented in Fig. 1 (compound **8**), Fig. 2 (compound **11**) and Fig. 3 (compound **6**). Cif files are given in supporting information and have been deposited at the Cambridge Crystallographic Data Centre (deposition numbers CCDC 230809–230811). In all three compounds, coordination about the B atom is almost tetrahedral. Coordination about the Fe centre is typical of ''half sandwich'' mono(cyclopentadienyl)metal complexes [26,27]. The X-ray crystal structure determinations confirm that for both compounds **8** and **11**, the oxygens of the initial acyl groups are connected through a C–O–B system with O–B of 1.559(3) Å, **8** and 1.570(3) Å, **11**, and C–O of 1.297(3), **8** and 1.254(3) Å, **11**. The attachment of the B(C_6F_5)$_3$ lengthens the original double acyl carbonyl bond and shortens the Fe–C(acyl) bond. The Fe–C(acyl) and (acyl)C=O bond lengths in the adduct **8** (1.904(2) and 1.297(3) Å, respectively) are intermediate between those found in typical Fe-acyl compounds (i.e. [Fe(η-C_5H_5)($COCH_3$)(CO){PPh_3}], [24] with Fe–C(acyl) bond 1.917(8) Å, (acyl)C=O bond 1.234(7) Å and [Fe(η-C_5H_5)($COCH_3$)(CO){$PPhMe_2$}] [25] with Fe–C bond 1.948(4) Å, (acyl)C=O bond 1.214(4) Å) and Fischer-carbenes (i.e. [Fe(η-C_5H_5)I{Ph-C(OEt)}(CO)] [26] with Fe–C bond 1.849(10) Å,

Table 2
Selected bond lengths (Å) and angles (°) for compounds **6**, **8** and **11**

Compound	Bond lengths		Bond angles	
6	O(1)–B(1)	1.508(2)	O(1)–Fe(1)–P(1)	92.13(4)
	Fe(1)–O(1)	2.0403(13)	C(19)–Fe(1)–P(1)	89.29(6)
	O(1)···F(1)	2.768(2)	O(1)–B(1)–C(1)	112.83(14)
	O(1)···F(15)	2.762(2)	C(1)–B(1)–C(7)	104.72(14)
			Fe(1)–O(1)–H(1)	109.4(20)
			B(1)–O(1)–H(1)	112.9(20)
			Fe(1)–O(1)–B(1)	136.83(11)
			O(1)–Fe(1)–C(19)	97.42(7)
8	Fe(1)–C(90)	1.745(3)	C(10)–Fe(1)–P(1)	92.55(8)
	Fe(1)–C(10)	1.904(2)	C(10)–Fe(1)–C(90)	94.36(13)
	Fe(1)–P(1)	2.185(8)	C(90)–Fe(1)–P(1)	90.76(11)
	C(10)–O(2)	1.297(3)		
	O(2)–B(1)	1.559(3)		
11	Fe(1)–C(8)	1.919(2)	C(8)–O(3)–B(1)	138.11(18)
	C(8)–O(3)	1.254(3)	C(1)–Fe(1)–C(8)	89.7(1)
	O(3)–B(1)	1.570(3)	O(3)–B(1)–C(16)	114.48(18)
	Fe(1)–C(1)	1.774(3)		
	Fe(1)–C(2)	1.763(3)		

(acyl)C═O bond 1.344(14) Å). Similarly, for **11** the Fe(1)–C(8) distance is 1.919(2) and (acyl)C═O is 1.254(3) Å.

The ORTEP diagram showing the molecular structure of **6** is given in Fig. 3. There are only three previously structurally characterised examples of coordinated $[HOB(C_6F_5)_3]$ [27–29]. $[PtMe\{HOB(C_6F_5)_3\}(bipy)]$ [28] and $[InMe\{HOB(C_6F_5)_3\}\{1,2\text{-}(N^iPr)_2C_8H_5\}]$ [29] are believed to be formed by analogous reaction pathways to that proposed above, due to the presence of adventitious H_2O. The B–O bond length in the free anion $[HOB(C_6F_5)_3]^-$ increases upon coordination to a metal centre from 1.487(3) in $[NEt_4][HOB(C_6F_5)_3]$ to 1.508(2) Å in **6**, 1.526(3) Å in $[PtMe\{HOB(C_6F_5)_3\}(bipy)]$ or 1.528(3) Å in $[InMe\{HOB(C_6F_5)_3\}\{1,2\text{-}(N^iPr)_2C_8H_5\}]$. The structure of **6** shows a weak interaction of the hydroxyl proton with the two fluorine atoms F(1) and F(15). The O atom is relatively close to one fluorine atom of two of the pentafluorophenyl groups (O(1)···F(1) 2.768(2) Å, O(1)···F(15) 2.762(2) Å). The hydroxyl group does not project directly towards either F and it is thus not clear whether any hydrogen bond is present. However, they cause the slight elongation of the corresponding C–F bonds to 1.362(2) and 1.361(2) Å, compared to the average of ca. 1.35 Å.

2.4. DFT calculations

Electronic structure calculations were undertaken to investigate the causes of the bond length changes on coordination of $B(C_6F_5)_3$. Consideration of resonance structures for the Lewis acid coordinated iron-acyl compound would suggest that the coordination decreases the double bond character of the C–O bond and increases that of the Fe–C bond. Such resonance structures are normally taken to imply a shift of π electrons (Scheme 4). To reduce computational time, in modelling the $B(C_6F_5)_3$ derivatives all C_6F_5 groups were substituted by fluorine atoms and C_6H_5 groups by hydrogen. Though in the isolated molecules the bonding in planar BF_3 and $B(C_6F_5)_3$ differs, in that the former has a strong π component, when tetrahedrally coordinated the B–F π bonding in BF_3 is considerably reduced. Such a substitution has been used successfully in a number of studies [21,30]. Geometry optimisations were carried out for the iron-acyl species: $[Fe(C_5H_5)(MeCO)(CO)_2]$ (**I**), $[Fe(C_5H_5)(MeCO)(CO)(PH_3)]$ (**II**) and $[Fe(C_5H_5)(MeCO)(CO)(PMe_3)]$ (**III**), and for their respective Lewis acid adducts: $[Fe(\eta\text{-}C_5H_5)\{MeCOBF_3\}(CO)_2]$ (**I′**), $[Fe(C_5H_5)\{MeCOBF_3\}(CO)(PH_3)]$ (**II′**) and $[Fe(C_5H_5)\{MeCOBF_3\}(CO)(PMe_3)]$ (**III′**). Fragment analyses were performed to analyze the bonding between the iron centre and the acyl carbon atom. $[Fe(\eta\text{-}C_5H_5)(MeCO)(CO)(L)]$ (L = CO and PMe_3) were split into $[Fe(\eta\text{-}C_5H_5)(CO)(L)]$ and [MeCO] and $[Fe(\eta\text{-}C_5H_5)(MeCOBF_3)(CO)(L)]$ into $[Fe(\eta\text{-}C_5H_5)(CO)(L)]$ and $[MeCOBF_3]$.

The results of all geometry optimisations are given in Table 4 together with experimental (X-ray diffraction) values for comparison. Reasonable agreement between calculated and experimental distances confirms that, in general, replacement of $B(C_6F_5)_3$ with BF_3, and that of PPh_3 with PH_3 provided accurate models. Table 5 shows the total energy gain upon coordination of BF_3 to Fe-acyls. The gas phase formation of O-acyl coordinated BF_3-adducts was found to be energetically favourable in all cases. The binding energy increases with the donor character of L. Examination of bond lengths

Table 3
Crystallographic data for compounds **6**, **8** and **11**

	6	**8**	**11**
Chemical formula	$C_{49}H_{29}BF_{15}FeO_2P$	$C_{29}H_{17}BF_{15}FeO_2P$	$C_{27}H_8BF_{15}FeO_3$
Formula weight	1032.37	780.05	731.99
Temperature (K)	150	150	150
Wavelength (Å)	0.71073	0.71073	0.71073
Crystal system	Triclinic	Monoclinic	Monoclinic
Space group	$P\bar{1}$	$P2_1/n$	$C2/c$
a (Å)	10.5856(3)	a = 12.1985(2)	26.3586(3)
b (Å)	14.0834(4)	b = 18.6027(3)	12.9606(2)
c (Å)	16.0926(5)	c = 13.4403(2)	19.6149(3)
α (°)	94.7028(10)	90	90
β (°)	108.2310(11)	102.8671(8)°	128.3594(7)
γ (°)	107.8446(12)	90	90
Cell volume (Å^3)	2126.7	2973.4	5254.4
Z	2	4	8
Calculated density (Mg/m^3)	1.612	1.742	1.851
Absorption coefficient (mm^{-1})	0.501	0.685	0.713
F_{000}	1041.305	1552	2884.362
Crystal size (mm)	$0.08 \times 0.14 \times 0.16$	$0.42 \times 0.2 \times 0.1$	$0.08 \times 0.12 \times 0.22$
Absorption correction	Semi-empirical from equivalent reflections	Semi-empirical from equivalent reflections	Semi-empirical from equivalent reflections
Transmission coefficients (min and max)	0.92 and 0.96	0.87 and 0.93	0.85, 0.94
θ Range for data collection (°)	$5.0 \leqslant \theta \leqslant 27.5$	$3.6 \leqslant \theta \leqslant 27.5$	$5.0 \leqslant \theta \leqslant 27.5$
Index ranges	$-13 \leqslant h \leqslant 12$, $-18 \leqslant k \leqslant 18$, $0 \leqslant l \leqslant 20$	$-15 \leqslant h \leqslant 15$, $-21 \leqslant k \leqslant 24$, $-17 \leqslant l \leqslant 17$	$-34 \leqslant h \leqslant 26$, $0 \leqslant k \leqslant 16$, $0 \leqslant l \leqslant 25$
Reflections measured	28,893	13,012	41,307
Unique reflections	9645	6809	6227
R_{int}	0.035	0.020	0.042
Observed reflections ($I > 3\sigma(I)$)	7198	4509	4348
Refinement method	Full-matrix least-squares on F	Full-matrix least-squares on F	Full-matrix least-squares on F
Parameters refined	626	550	424
Weighting scheme	Chebychev 3-term polynomial	Chebychev 3-term polynomial	Chebychev 3-term polynomial
Goodness-of-fit	1.0461	1.0199	1.0425
R_1	0.0348	0.0406	0.0369
wR_2	0.0397	0.0492	0.0419
Residual electron density (min and max) (e Å^{-3})	−0.35, 0.41	−0.38 and 0.66	−0.40, 0.57

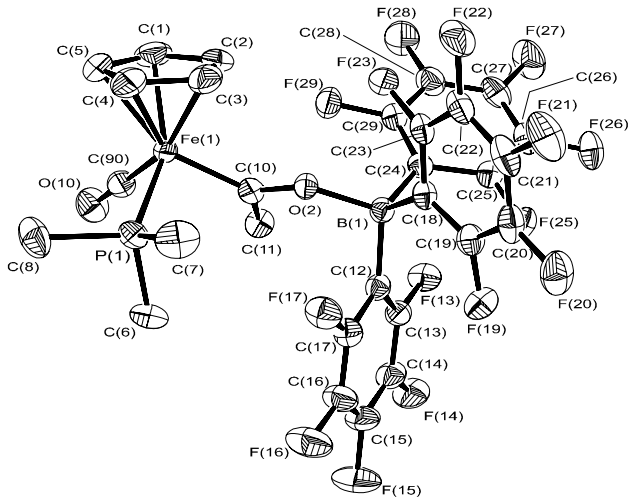

Fig. 1. ORTEP of compound **8**.

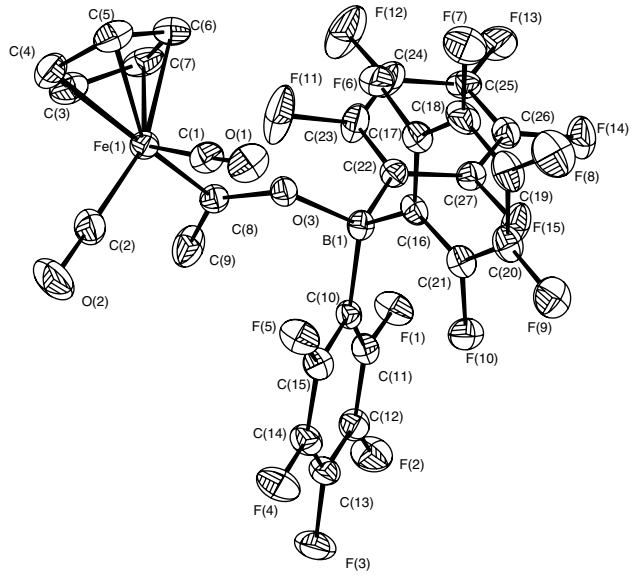

Fig. 2. ORTEP of compound **11**.

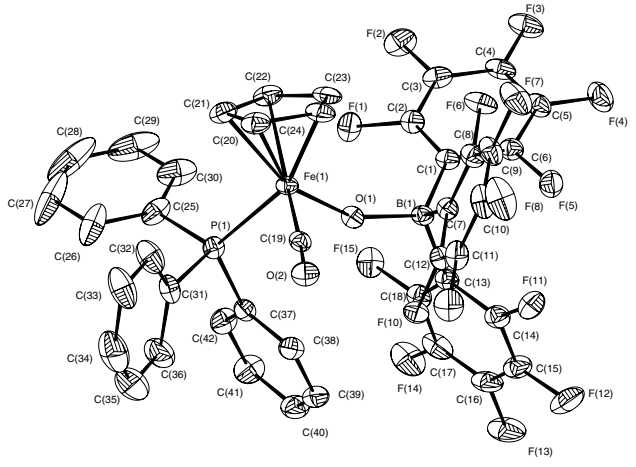

Fig. 3. ORTEP of compound **6**.

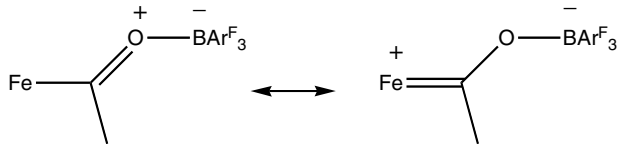

Scheme 4. Resonances structures for [Fe(η-C_5H_5){MeCOB(C_6F_5)$_3$}(CO)(L)].

shown in Table 4 shows that the acyl C–O distances increase upon coordination by BF_3 (0.05 Å on average) and Fe–C (acyl bond) shortens by an average of 0.06 Å compared with parent acyl compound. The O–B distances in the Fe-(μ-CO)B unit show significant variation in the order L = CO > PH_3 > PMe_3 and the B–F distances correlate inversely with the B–O distances. Compounds **I**, **I′**, **III** and **III′** were chosen for fragment analysis, as these represent the electronic extremes for the system. The movement of charge on coordination of BF_3 is shown in Fig. 4. The charge on the [Fe(η-C_5H_5)(CO)(L)] fragment is positive and is greater for L = PMe_3 than L = CO. On binding BF_3 there is a transfer of electron density from both the Fe centre and the acyl fragment, towards the BF_3 moiety. There is thus a correlation between the charge transfer and the binding energy, both increasing with the donor power of L.

The HOMO of [Fe(η-C_5H_5)(MeCO)(CO)(L)] is shown in Fig. 5 for L = CO and PMe_3. In both cases the HOMO is the principal Fe-acyl bonding orbital. However it is not localised in the Fe–C bond but has a contributions from the O pπ orbital lying in the acyl plane and from the C–Me bond. The six Fe d electrons occupy the next three orbitals. It is the HOMO that is the source of the electron pair donation to the Lewis acidic BF_3 and O that acts as the donor atom. Consequently the O–B bond is formed in the plane of the acyl group and at an angle of ca. 125° to the C–O bond. Binding of the acyl group to [Fe(η-C_5H_5)(CO)(L)] involves principally the acyl HOMO and to a certain extent its LUMO. As the acyl group is planar the orbitals may be classified as σ for the HOMO and π for the LUMO. The HOMO has an outward pointing lobe directed towards the Fe but also has a contribution from the O p orbital in the C–C–O plane. The acyl HOMO is C–O antibonding. The LUMO is a π* C–O antibonding orbital (Scheme 5).

Orbital occupancies for the acyl HOMOs and LUMOs in [Fe(η-C_5H_5)(MeCO)(CO)(L)] are given in Table 6. When L = CO the acyl HOMO has an occupancy of 1.0 electrons and the LUMO one of 0.09 electrons, indicating little π bonding by the Fe centre to the acyl ligand. For L = PMe_3 both the HOMO and LUMO occupancy are slightly greater at 1.1 and 0.19 respectively. As both the acyl HOMO and LUMO are C–O antibonding the C–O distance is longer in **III** than **I**

Table 4
Selected distances (Å) and angles (°) calculated for **I-III**, **I′-III′**

Compound	Fe–C (acyl)	Fe–P	Fe–C (carbonyl)	O=C (acyl)	B–O (acyl)	C≡O	B–F	Fe–C(acyl)–O	Fe–C(acyl)–C	C(acyl)–O–B
I	1.958		1.725, 1.722	1.206		1.156, 1.160		122.2	116.6	
II	1.932	2.216	1.715	1.213		1.161		124.3	117.2	
III	1.914	2.137	1.705	1.226		1.164		126.0	119.2	
I′	1.891		1.734, 1.732	1.253	1.593	1.149, 1.154	1.352, 1.371, 1.378	119.4	119.1	124.2
II′	1.869	2.121	1.722	1.263	1.571	1.156	1.355, 1.370, 1.378	120.5	121.6	124.5
III′.	1.850	2.156	1.710	1.276	1.546	1.160	1.360, 1.375, 1.380	121.0	122.9	125.3
[Fe(η-C_5H_5)(MeCO)-(CO)(PPh_3)][a]	1.917(8)	2.202(2)	1.708(8)	1.234(7)		1.171(6)		123.2(6)	122.8(2)	
[Fe(η-C_5H_5)(MeCO)-(CO)($PPhMe_2$)] [b]	1.948(4)	2.180(1)	1.725(4)	1.214(4)		1.161(4)		123.0(3)	120.7(3)	
[Fe(η-C_5H_5)I{PhC-(OEt)}(CO)][c]	1.849(10)		1.758(13)	1.344(14)		1.157(15)		133.4(6)	122.6(8)	
8	1.904(2)	2.185(8)	1.745(3)	1.297(3)	1.559(3)	1.155(4)		116.1(2)	122.77(17)	131.65(19)
11	1.919(2)		1.774(3) 1.763(3)	1.254(3)	1.570(3)	1.140(3) 1.142(3)		118.04(16)	122.13(16)	138.11(18)

Where available, experimental distances of related derivatives are given for comparison. Calculated Cp(C–C) and Fe–C(Cp) distances are all within expected range.
[a] Ref. [24].
[b] Ref. [25].
[c] Ref. [26].

Table 5
Estimated energy difference between [Fe-acyl] species **I–III** and their corresponding BF_3 adducts (**I′–III′**)

L	ΔE (kJ mol^{-1})
[Fe(η-C_5H_5)(MeCO)(CO)(L)] + BF_3 →[Fe(η-C_5H_5){$MeCOBF_3$}(CO)(L)]	
CO	−31
PH_3	−51
PMe_3	−67

Energy for free BF_3 ca. 210 kJ/mol, L = CO, PH_3, PMe_3.

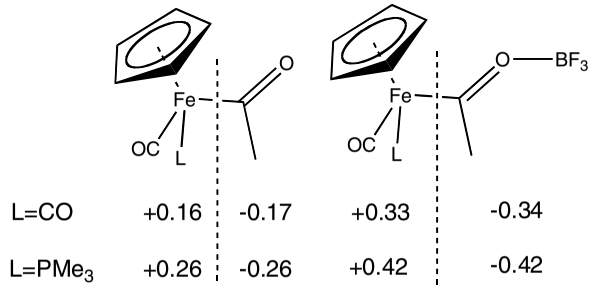

Fig. 4. Charges on fragments found from fragment analysis.

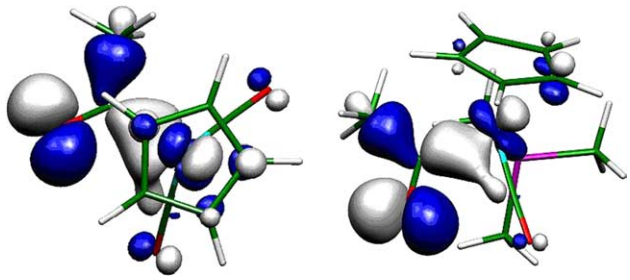

Fig. 5. HOMOs of [Fe(C_5H_5)(MeCO)($CO)_2$] and [Fe(C_5H_5)(MeCO)(CO)(PMe_3)].

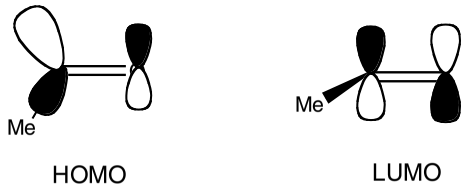

Scheme 5. HOMO and LUMO of the acyl fragment.

(Table 4). This lengthening is seen to be a combination of σ and π effects.

In the fragment [$MeCOBF_3$] the HOMO and LUMO are directly comparable to those of the acyl group. The HOMO is stabilised directly by the coordination of the BF_3 which binds in the C–C–O plane. The LUMO is also stabilized but is not involved directly in BF_3 bonding as it is orthogonal to the BF_3 acceptor orbital (Scheme 6). Addition of BF_3 to [Fe(η-C_5H_5)(MeCO)($CO)_2$] leads to an increase in the occupancy of the

Table 6
Occupancies of fragment MOs (FMOs) for **I**, **I′**, **III** and **III′**

Compound	Fragment	FMO	Occupancy
$[Fe(\eta\text{-}C_5H_5)(MeCO)(CO)_2]$ (**I**)	MeCO	HOMO	1.03
	MeCO	LUMO	0.09
	$Fe(\eta\text{-}C_5H_5)(CO)_2$	HOMO	1.03
$Fe(\eta\text{-}C_5H_5)\{MeCOBF_3\}(CO)_2]$ (**I′**)	$\{MeCOBF_3\}$	HOMO	1.25
	$\{MeCOBF_3\}$	LUMO	0.14
	$Fe(\eta\text{-}C_5H_5)(CO)_2$	HOMO	0.83
$[Fe(\eta\text{-}C_5H_5)(MeCO)(CO)(PMe_3)]$ (**III**)	MeCO	HOMO	1.13
	MeCO	LUMO	0.19
	$Fe(\eta\text{-}C_5H_5)(CO)(PMe_3)$	HOMO	0.92
$[Fe(\eta\text{-}C_5H_5)\{MeCOBF_3\}(CO)(PMe_3)]$ (**III′**)	$\{MeCOBF_3\}$	HOMO	1.3
	$\{MeCOBF_3\}$	LUMO	0.29
	$Fe(\eta\text{-}C_5H_5)$ $(CO)(PMe_3)$	HOMO	0.78

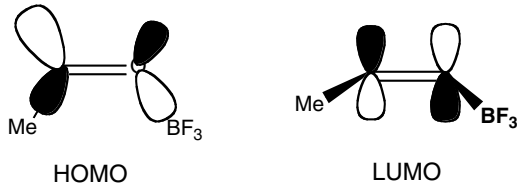

Scheme 6. HOMO and LUMO of the acyl-BF_3 fragment.

acyl-BF_3 HOMO from 1.0 to 1.2. The acyl-BF_3 LUMO also increases its occupancy to 0.14. This represents a movement of electron density from the metal. The shift is greater in the σ framework than in the π. When L = PMe_3 a similar shift occurs of 0.2 electrons in the σ system and 0.1 in the π. In both cases these shifts result in a lengthening of the CO bond and a shortening of the Fe–C bond on BF_3 coordination.

Thus the simple resonances structures, as presented, are deceptive in so far as they are taken to indicate shifts in π population. The bond length changes on BF_3 coordination are as much, if not more, due to changes in σ occupancy. The acyl σ HOMO is CO antibonding and increase in its occupancy increases the CO bond length.

3. Conclusions

The reactivity of $[Fe(\eta\text{-}C_5H_5)(MeCO)(CO)(L)]$ towards $B(C_6F_5)_3$ has been investigated. New complexes incorporating the [Fe-acyl-$B(C_6F_5)_3$] unit have been prepared, characterised and their electronic structure investigated. DFT calculations indicate that formation of O-acyl-coordinated adducts of BF_3 is thermodynamically favourable both the binding energy and the charge transfer increasing with the donor power of the other ligands bound to Fe. The lengthening of the C–O bond and shortening of the Fe–C bond on $B(C_6F_5)_3$ coordination is not precisely described by resonance structures, as it is shown to be a combination of both σ and π effects, both the σ HOMO and the π LUMO of the acyl group increasing their occupancy on BF_3 coordination and both and C–O antibonding. Thus π populations cannot be inferred from distance changes.

4. Experimental

All reactions were carried out under N_2, using conventional Schlenk-line techniques. The compounds $[Fe(\eta\text{-}C_5H_5)(Me)(CO)_2]$ [31], PMe_3 [32], $B(C_6F_5)_3$ [33], $[Fe(\eta\text{-}C_5H_5)(Me)(CO)(PPh_3)]$ [34], and $[Fe(\eta\text{-}C_5H_5)(Me)(CO)(PMe_3)]$ [35] (**2**) were prepared according to the literature methods. The compunds $[Fe(\eta\text{-}C_5H_5)(\mu\text{-}CO)_2(CO)]$, PPh_3, $PPhMe_2$, PPh_2Me, PCy_3, MeCOCl, MeI and alumina (activated, neutral, Brockmann I, Std Grade, 150 mesh) were purchased from Aldrich Chemical Co. and used as received. NMR spectra were recorded on either a 300 MHz Varian Mercury or a 500 MHz Varian Unity spectrometer, referenced internally using the residual protio-solvent, and chemical shifts were reported with respect to $SiMe_4$ (^1H and ^{13}C, $\delta = 0$), $BF_3 \cdot Et_2O$ (^{11}B, $\delta = 0$), H_3PO_4 (^{31}P, $\delta = 0$) and $CFCl_3$ (^{19}F, $\delta = 0$). All chemical shifts are quoted in δ (ppm) and coupling constants in Hz. Infrared spectra were recorded on either a Perkin–Elmer 1710 IR FT spectrometer or a Perkin–Elmer 1600 FTIR. GC–MS chromatographs and spectra were recorded using a Hewlett–Packard 5890 Gas Chromatograph fitted with a non-polar column connected to a Trio-1000 Mass Spectrometer operating Electron Impact (70 eV) and Chemical Ionisation (CI) mode (NH_3) and detecting positively charged species. The temperature profile for the GC is shown below. Elemental analyses and mass spectra were provided by the Microanalytical Services of the Inorganic Chemistry Laboratory, Oxford.

The spectroscopic data are: for [Fe(η-C_5H_5)(Me)(CO)(PPh_3)] **1**, IR (Nujol): 1902s, 1600s [C═O stretch].

NMR (C_6D_6): ^{1}H: 2.60 [3H, s, COCH_3], 4.28 [5H, d, ^3J(H,P) = 1.2 Hz, C_5H_5], ~7.06 [9H, m, *p*-/*m*-(C_6H_5)$_3$], 7.74 [6H, m, *o*-(C_6H_5)$_3$]. ^{13}C{^{1}H}: 51.6 [d, ^3J(C,P) = 6.4 Hz, CO*C*H$_3$], 85.4 [d, ^2J(C,P) = 0.8 Hz, *C*$_5$H$_5$], 128.2 [d, ^3J(C,P) = 9.7 Hz, *m*-(C_6H_5)$_3$], 129.8 [d, ^4J(C,P) = 2.3 Hz, *p*-(C_6H_5)$_3$], 133.8 [d, ^2J(C,P) = 9.4 Hz, *o*-(C_6H_5)$_3$], 137.4 [d, ^1J(C,P) = 42.4 Hz, *i*-(C_6H_5)$_3$], 221.2 [d, ^2J(C,P) = 31.3 Hz, *C*O], 269.5 [d, ^2J(C,P) = 23.0 Hz, *C*OCH$_3$]. ^{31}P{^{1}H}: 77.6 [s, *P*(C_6H_5)$_3$].

For [Fe(η-C_5H_5)(Me)(CO)(PMe_3)] (**2**) IR (Nujol): 1914 s, 1604 m [C═O Stretch]. NMR ($CDCl_3$): ^{1}H: 1.22 [9H, d, ^2J(P,H) = 9.7 Hz, P(CH_3)$_3$], 2.41 [3H, s, COCH_3], 4.35 [5H, s, C_5H_5]; ^{31}P{H}: 44.8 [s, *P*Me$_3$].

4.1. Preparation

4.1.1. *Fe(η-C_5H_5)(MeCO)(CO)($PPhMe_2$)] (**3**)*

$PPhMe_2$ (0.4 cm^3, 2 mmol) was added to a solution of [Fe(η-C_5H_5)(CH_3)(CO)$_2$] (0.35 g, 2 mmol) in toluene (10 cm^3) and refluxed under N_2 for 2 h. The solvent was removed under reduced pressure and the resultant solid purified by chromatography on silica. The first fraction (yellow) was collected with light petrol and the second (orange) with 50% diethyl ether and 50% tetrahydrofuran. The solvent was removed from the second fraction, the product extracted from light petrol and then dried under reduced pressure to give [Fe(η-C_5H_5)(MeCO)(CO)($PPhMe_2$)] as an orange-brown solid. Yield: 30%. Elemental Analysis: $C_{11}H_{17}FeO_2P$ Found (Calc.) %C 49.4 (49.3), %H 6.7 (6.4), %P 10.1 (11.6). IR (Nujol): 1916 s, 1605 m [C═O Stretch].

NMR (d^8-toluene): ^{1}H: 1.41 [3H, d, ^1J(P,H) = 8.7 Hz, P(CH_3)$_2$], 2.48 [3H, s, COCH_3], 4.31 [5H, s, C_5H_5], 7.32 [3H, s, *m*-/*p*-C_6H_5], 7.48 [2H, s, *o*-C_6H_5]; ^{31}P{^{1}H}: 52.0 [s, *P*PhMe$_2$].

4.1.2. *Fe(η-C_5H_5)(MeCO)(CO)(PCy_3)] (**4**)*

The procedure described for the synthesis of **3** was followed, using PCy_3 (4.2 g, 10 mmol) and [Fe(η-C_5H_5)(CH_3)(CO)$_2$] (1.95 g, 15 mmol) to give [Fe(η-C_5H_5)(COCH_3)(CO)(PCy_3)] as a yellow-brown solid. Yield: 70%. IR (Nujol): 1914 s, 1623 m [C═O Stretch].

NMR (d^8-toluene): ^{1}H: 2.51 [33H, m, P(C_6H_{11})$_3$], 2.58 [3H, s, COCH_3], 4.53 [5H, s, C_5H_5]; ^{31}P{H}: 75.3 [s, *P*Cy$_3$].

4.1.3. *Fe(η-C_5H_5)(MeCO)(CO)$_2$] (**5**)*

[Fe_2(η-C_5H_5)$_2$(μ-CO)$_2$(CO)$_2$] (3.54 g, 10 mmol) in THF (50 cm^3) was added to ~3% sodium amalgam (0.98 g, 0.021 mol Na + 35 g Hg) and occasionally swirled over three hours. The solution was then filtered in to another flask and cooled to −78 °C before CH_3COCl (1.6 ml, 10 mol) was added dropwise with stirring. The mixture was left at −78 °C for 20 min then left to return to room temperature. Solvent was then removed under reduced pressure, the resulting oil dissolved in toluene and filtered. Drying under reduced pressure gave [Fe(η-C_5H_5)(MeCO)(CO)$_2$] as a yellow-brown powder that was purified by sublimation (52 °C and 0.1 bar). Yield 40%. IR (Nujol): 2023 s, 1956 s, 1656 m [C═O Stretch].

NMR (d^8-toluene): ^{1}H: 2.37 [3H, s, COCH_3], 4.68 [5H, s, C_5H_5].

4.1.4. *[Fe(η-C_5H_5){MeCOB(C_6F_5)$_3$}(CO)(PPh_3)] (**7**) and [Fe(η-C_5H_5){HOB(C_6F_5)$_3$}(CO)(PPh_3)] (**6**)*

NMR scale. A solution of B(C_6F_5)$_3$ (0.017 g, 0.033 mmol) in C_6D_6 was added dropwise to a solution of [Fe(η-C_5H_5)(MeCO)(CO)(PPh_3)] (0.015 g, 0.033 mmol) in C_6D_6. The combined solution was transferred to a Young's Tap NMR tube and monitored by ^{1}H, ^{19}F, ^{31}P and ^{11}B NMR spectroscopy.

Preparative scale. A solution of B(C_6F_5)$_3$ (0.225 g, 0.44 mmol) in toluene (20 cm^3) was added dropwise, with stirring, over 10 min to a solution of [Fe(η-C_5H_5)(CH_3CO)(CO)(PPh_3)] (200 mg, 0.44 mmol) in toluene (20cm^3) at −78°C. The orange mixture was stirred for 1 h at −78°C. The cooling bath was removed and the solution allowed to warm to room temperature whilst stirring for a further hour. Removal of solvents yielded [Fe(η-C_5H_5){MeCOB(C_6F_5)$_3$}(CO)(PPh_3)], (**7**), as a yellow solid. Yield: 99%. Elemental Analysis: Found (Calculated) %C 54.7 (54.7), %H 2.9 (2.4) IR (Nujol): 1957s, 1517m [C═O stretch]. NMR (d^8-toluene): ^{1}H: 2.21 [3H, s, COCH_3], 4.18 [5H, s, C_5H_5], 7.00 [9H, s, *m*-/*p*-C_6H_5], 7.22 [6H, s, *o*-C_6H_5]; ^{13}C{H}: 49.82 [1C, s, CO*C*H$_3$], 87.12 [5C, s, *C*$_5$H$_5$], 130.76 [6C, s, *m*-*C*$_6$H$_5$], 133.60 [3C, s, *p*-*C*$_6$H$_5$], 134.20 [6C, s, *o*-*C*$_6$H$_5$], 133.24 [3C, s, *i*-*C*$_6$H$_5$]; 218.01[1C, d, ^2J(P,C) = 28.7 Hz, *C*O].

^{19}F: −167.1 [6F, td ^3J(F,F) = 21.1 Hz ^4J(F,F) = 5.6 Hz, *m*-C_6F_5], −160.9 [3F, t ^3J(F,F) = 21.09 Hz, *p*-C_6F_5], −134.0 [6F, d ^3J(F,F) = 16.9 Hz, *o*-C_6F_5]; ^{31}P{^{1}H}:67.3 [s, *P*Ph$_3$]; ^{11}B{^{1}H}: −14.0.

FAB$^+$. *m/z* (Intensity %), [Assignment]: 411 (9), [Fe(PPh_3)(C_5H_5)(CO)]$^+$, 383 (100), [Fe(PPh_3)(C_5H_5)]$^+$, 121 (20), [Fe(C_5H_5)$^+$].

Attempted purification of [Fe(η-C_5H_5){CH_3 COB(C_6F_5)$_3$}(CO)(PPh_3)] by chromatography on silica in THF led only to formation of the hydrolysis product [Fe(η-C_5H_5){HOB(C_6F_5)$_3$}(CO)(PPh_3)] (**6**). Yield 20%. IR (Nujol): 3229 m [H-O stretch], 1973 s [C≡O stretch] NMR (d^8-toluene): ^{1}H: 2.00 [3H, s, COCH_3], 3.84 [5H, s, C_5H_5], 7.00 [9H, s, *m*-/*p*-C_6H_5], 7.13 [6H, s, *o*-C_6H_5]; ^{19}F: −165.5 [6F, td ^3J(F,F) = 22.6 Hz ^4J(F,F) = 5.6 Hz, *m*-C_6F_5], −156.92 [3F, s, *p*-C_6F_5], −141.34 [6F, s, *o*-C_6F_5]; ^{31}P: 68.6 [s, *P*Ph$_3$].

Mass Spec.(EI+) *m/z*(Intensity %) [Assignment]: 612(10) [Fe{HOB(C_6F_5)$_3$}(CO)]$^+$, 528(10) [HOB(C_6F_5)$_3^+$], 383(100) [Fe(C_5H_5)(PPh_3)]$^+$.

4.1.5. Fe(η-C_5H_5){MeCOB(C_6F_5)$_3$}(CO)(PMe_3) (**8**)

NMR scale. A solution of B(C_6F_5)$_3$ (0.029 g, 0.056 mmol) in C_6D_6 was added dropwise to a solution of [Fe(η-C_5H_5)($COCH_3$)(CO){$P(CH_3)_3$}] (0.015 g, 0.056 mmol) in C_6D_6. The combined solution was transferred to a Young's tap NMR tube and monitored by ^{1}H, ^{19}F, ^{31}P{^{1}H} and ^{11}B{^{1}H} NMR spectroscopy.

Preparative scale. This synthesis was performed in the same manner as described for **7**, using [Fe(η-C_5H_5)(MeCO)(CO)(PMe_3)] (0.134 g, 5 mmol) and B(C_6F_5)$_3$ (0.256 g, 5 mmol). [Fe(η-C_5H_5){MeCOB(C_6F_5)$_3$}(CO)(PMe_3)] was obtained as a green powder. Yield 85%. Elemental Analysis: Found (Calculated) %C 44.4 (44.6), %H 2.6 (2.2). IR (Nujol): 1948 s [C≡O stretch], 1520 m [C═O stretch] NMR (d^8-toluene): ^{1}H: 0.81 [9H, d ^1J(H,P) = 6.8 Hz, P(CH_3)$_3$], 2.34 [3H, s, COCH_3], 3.98 [5H, d ^3J(H,P) = 2 Hz, C_5H_5]; ^{11}B: −13.9; ^{19}F: −164.1 [6F, td ^3J(F,F) = 22.5 Hz ^4J(F,F) = 11.3 Hz, *m*-C_6F_5], −157.5 [3F, t ^3J(F,F) = 21.2 Hz, *p*-C_6F_5], −133.2 [6F, d ^3J(F,F) = 22.5 Hz, *o*-C_6F_5]; ^{31}P{H}: 43.1 [s, $P(CH_3)_3$]. FAB$^+$: *m/z* (Intensity %) [Assignment]: 585(3) [Fe (C_5H_5){MeCOB(C_6F_5)$_3$}(PMe_3)]$^+$, 444(2) [Fe(C_5H_5){MeCOB(C_6F_5)$_3$}(PMe_3)]$^+$.

4.1.6. [Fe(η-C_5H_5){MeCOB(C_6F_5)$_3$}(CO)($PPhMe_2$)] (**9**)

This synthesis was performed in the same manner as described for **7**, using [Fe(η-C_5H_5)(MeCO) (CO)($PPhMe_2$)] (0.165 g, 5 mmol) and B(C_6F_5)$_3$ (0.256g, 5 mmol). [Fe(η-C_5H_5){MeCOB(C_6F_5)$_3$}(CO)($PPhMe_2$)] was obtained as a green-brown powder. Yield: 89%.

Elemental Analysis: Found (Calculated) %C 47.93 (48.46), %H 2.90 (2.26)IR (Nujol): 1952 s [C≡O stretch], 1518 m [C═O stretch]. NMR (d^8-toluene): ^{1}H: 1.85 [6H, d ^1J(P,H) = 14 Hz, P(CH_3)$_2$], 2.09 [3H, s, COCH_3], 3.73 [5H, s, C_5H_5], 6.78 [3H, s, *m*-/*p*-C_6H_5], 6.88 [2H, s, *o*-C_6H_5]; ^{19}F: −172.49 [6F, *m*-C_6F_5], −165.83 [3F, t 3J(F,F) = 20.2 Hz, *p*-C_6F_5], −139.9 [6F, d 3J(F,F) = 21.3 Hz, *o*-C_6F_5]; ^{31}P{H}:36.7 [s, PPhMe$_2$].

4.1.7. Fe(η-C_5H_5){MeCOB(C_6F_5)$_3$}(CO)(PCy_3)] (**10**)

This synthesis was performed in the same manner as described for **7**, using [Fe(η-C_5H_5)(MeCO)(CO)(PCy_3)] (0.236 g, 5 mmol) and B(C_6F_5)$_3$ (0.256 g, 5 mmol). [Fe(η-C_5H_5){MeCOB(C_6F_5)$_3$}(CO)(PCy_3)] was obtained as a yellow-brown powder. Yield: 85%.

Elemental Analysis: Found (Calculated) %C 54.0 (53.7), %H 5.0 (4.2). IR (Nujol): 2048 s 2005 s [C≡O stretches], 1509 m [C═O stretch]. NMR (d^8-toluene): ^{1}H: 1.52 [33H, broad m, P(C$_6H_{11}$)$_3$], 2.72 [3H, s, COCH_3], 4.23 [5H, s, C_5H_5]; ^{13}C{H}: 26.5 27.6 30.8 31.0 [18C, s, P(C$_6H_{11}$)$_3$], 41.2 [1C, s, CO*C*H3], 86.2 [5C, s, C_5H_5], 126 [3C, s, *i*-C_6F_5], 128 [3C, *m*-C_6F_5], 129 [6C, *p*-C_6F_5], 136 [6C, *o*-C_6F_5]; ^{11}B{^{1}H}: −14.1; ^{19}F: −170.0 [6F, d ^3J(F,F) = 22.6 Hz, *m*-C_6F_5], −167.5 [3F, s, *p*-C_6F_5], −133.5 [6F, d ^3J(F,F) = 22.6 Hz, *o*-C_6F_5]; ^{31}P{H}: 80.1 [s, PCy_3]. FAB$^+$: *m/z* (Intensity %) [Assignment]: 984(1) [Fe(C_5H_5){MeCOB(C_6F_5)$_3$}(CO)-(PCy_3)]$^+$, 401(97) [Fe(MeCO)(CO)(PCy_3)]$^+$.

4.1.8. [Fe(η-C_5H_5){MeCOB(C_6F_5)$_3$}(CO)$_2$] (**11**)

This synthesis was performed in the same manner as described for **7**, using [Fe(η-C_5H_5)(MeCO)(CO)$_2$] (0.110 g, 5 mmol) and B(C_6F_5)$_3$ (0.256 g, 5 mmol). [Fe(η-C_5H_5){MeCOB(C_6F_5)$_3$}(CO)$_2$] was obtained as a green powder, with 92% yield. Elemental Analysis: Found (Calculated) %C 44.1 (44.3), %H 1.3 (1.1). IR (Nujol): 2052 s 1994 s [C≡O stretch], 1517 m [C═O stretch]. NMR (d^8-toluene): ^{1}H: 2.04 [3H, s, COCH_3], 3.88 [5H, s, C_5H_5]; ^{13}C{H}:44.8 [1C, s, CO*C*H3], 89.1 [5C, s, C_5H_5]; ^{19}F: −163.8 [6F, td ^3J(F,F) = 22.7 Hz ^4J(F,F) = 7.3 Hz, *m*-C_6F_5], −156.9 [3F, t, ^3J(F,F) = 20.5 Hz, *p*-C_6F_5], −134.5 [6F, d ^3J(F,F) = 20.9 Hz, *o*-C_6F_5] FAB$^+$: *m/z* (Intensity %) [Assignment]: 665(19), [Fe(CO)$_2${MeCOB(C_6F_5)$_3$}]$^+$, 221(88) [Fe(C_5H_5)(MeCO)(CO)$_2$]$^+$.

4.1.9. X-ray crystallography

In each case, a single crystal was selected under inert atmosphere, encased in perfluoro-polyether oil, and mounted on the end of a glass fibre. The fibre, secured on a goniometer head was then placed under a stream of cold nitrogen maintained at 150 K. Data was collected on an Enraf-Nonius DIP2000 image plate diffractometer (complex **8**) or a Nonius KCCD diffractometer (complexes **6** and **11**), using graphite monochromated Mo Kα radiation (λ = 0.71069 Å). The images were processed with the DENZO and SCALEPACK programs[32]. Corrections for Lorentz and polarisation effects were performed. All solution, refinement, and graphical calculations were performed using the CRYSTALS [36] and CAMERON [37] software packages. The structures were solved by direct methods using the SIR92 [38] program and refined by full-matrix least squares procedure on *F*. All non-hydrogen atoms were refined with anisotropic displacement parameters. All hydrogen atoms were generated and allowed to ride on their corresponding carbon atoms with fixed thermal parameters. An empirical absorption correction was applied [38]. The crystallographic data are summarised in Table 3. The crystal structure of **8** was modelled as disordered over two positions, with refined occupancies. A 9:1 distribution of the two enantiomers of **8** suggests that disorder arises in the crystal packing when 10% of one enantiomer occupies sites usually occupied by the other enantiomer, and vice-versa.

5. DFT calculations

ADF calculations were performed using Vosko, Wilke and Nusair's local functional [39], with the Becke 88 [40] and the Perdew 86 [41] non local exchange and correlation gradient corrections, on ADF version 2000.02 [42–45]. The basis sets used were uncontracted triple-ξ Slater-type orbitals (STOs). The cores of atoms were frozen, B, C, O and F up to the 1s level, P and Fe up to the 2p level. Fragment calculations were carried out in order to separate the σ and π contributions to the Fe-acyl bonding. Charge analysis of the fragments was carried out by Mulliken, Voronoi or Hirschfeld partitioning [46]. The values given in Fig. 4 are those resulting from the Hirschfeld method.

6. Cambridge database deposit numbers

CCDC 230809; CCDC 230810; CCDC 230811.

Acknowledgements

We thank Dr. Neale G. Jones for helpful discussions, the Oxford Supercomputing Centre for use of its facilities, Balliol College Oxford for a Dervorguilla Scholarship (S.I.P), the AG Leventis Foundation (I.C.V) and EPSRC for support.

References

[1] A.C. Vosloo, Fuel Process. Technol. 71 (2001) 149.
[2] C. Masters, Adv. Organomet. Chem. 17 (1979) 61.
[3] A.R. Cutler, P.K. Hanna, J.C. Vites, Chem. Rev. 88 (1988) 1363.
[4] R.T. Aplin, J. Booth, R.G. Compton, S.G. Davies, S. Jones, J.P. McNally, M.R. Metzler, W.C. Watkins Soc., J. Chem. Perkin Trans. 2 (1999) 913.
[5] L.S. Liebeskind, M.E. Welker, Organometallics 2 (1983) 194.
[6] J.-P. Barras, S.G. Davies, M.R. Metzler, A.J. Edwards, V.M. Humphreys, K. Prout, J. Organomet. Chem. 461 (1993) 157.
[7] S.G. Davies, Aldrichimica 23 (1990) 31.
[8] P.M. Treichel, R.L. Shubkin, Inorg. Chem. 6 (1967) 1328.
[9] J.A. Van Doorn, C. Masters, H.C. Volger, J. Organomet. Chem. 105 (1976) 245.
[10] S.G. Davies, S.J. Simpson, S.E. Thomas, J. Organomet. Chem. 254 (1983) C29.
[11] M. Akita, O. Mitani, M. Sayama, Y. Morooka, Organometallics 10 (1991) 1394.
[12] M.L.H. Green, L.C. Mitchard, M.G. Swanwick, J. Chem. Soc. A (1971) 794.
[13] G.J. Baird, S.G. Davies, T.R. Maberly, Organometallics 3 (1984) 1764.
[14] R.E. Stimson, D.F. Shriver, Inorg. Chem. 19 (1980) 1141.
[15] D.J. Parks, J.M. Blackwell, W.E. Piers, J. Org. Chem. 65 (2000) 3090.
[16] T.C. Forschner, A.R. Cutler, Inorg. Synth. 26 (1989) 231.
[17] M. Green, D.J. Westlake, J. Chem. Soc. A (1971) 367.
[18] M.L.H. Green, J. Haggitt, C.P. Mehnert Soc., J. Chem. Chem. Commun. (1995) 1853.
[19] A.A. Danopoulos, J.R. Galsworthy, M.L.H. Green, L.H. Doerrer, S. Cafferkey, M.B. Hursthouse Soc., J. Chem. Chem. Commun. (1998) 2529.
[20] M.N. Golovin, M.M. Rahman, J.E. Belmonte, W.P. Giering, Organometallics 4 (1985) 1981.
[21] I.C. Vei, S.I. Pascu, M.L.H. Green, J.C. Green, R.E. Schilling, G.D.W. Anderson, L.H. Rees, Dalton Trans. (2003) 2550.
[22] S.J. Lancaster, D.A. Walker, M. Thornton-Pett, M. Bochmann, J. Chem. Soc., Chem. Commun. (1999) 1533.
[23] J. Zhou, S.J. Lancaster, D.A. Walker, S. Beck, M. Thornton-Pett, M. Bochmann, J. Am. Chem. Soc. 123 (2001) 223.
[24] H.Y. Liu, L.L. Koh, K. Eriks, W.P. Giering, A. Prock, Acta Crystallogr., Sect. C C46 (1990) 51.
[25] H.Y. Liu, K. Eriks, W.P. Giering, A. Prock, Acta Crystallogr., Sect. C C48 (1992) 433.
[26] H. Adams, N.A. Bailey, C. Ridgway, B.F. Taylor, S.J. Walters, M.J. Winter, J. Organomet. Chem. 394 (1990) 349.
[27] A. Spannenberg, V.V. Burlakov, P. Arndt, W. Baumann, V.B. Shut, U. Rosenthal, Z. Kristallogr, New Cryst. Struct. 217 (2002) 546.
[28] G.S. Hill, L. Manojlovic-Muir, K.W. Muir, R.J. Puddephatt, Organometallics 16 (1997) 525.
[29] I.A. Guzei, F. Delpech, R.F. Jordan, Acta Crystallogr., Sect. C C56 (2000) E327.
[30] J.R. Galsworthy, J.C. Green, M.L.H. Green, M. Muller, J. Chem. Soc., Dalton Trans. (1998) 15.
[31] T.S. Piper, G. Wilkinson, J. Inorg. Nucl. Chem. 3 (1956) 104.
[32] M.L. Luetkens, Jr., A.P. Sattelberger, H.H. Murray, J.D. Basil, J.P. Fackler Jr., Inorg. Synth. 28 (1990) 305.
[33] J.L.W. Pohlmann, F.E. Brinckman, Z. Naturforsch. 20 (1965) 5.
[34] M.L.H. Green, C.R. Hurley, J. Organomet. Chem. 10 (1967) 188.
[35] P.M. Treichel, D.A. Komar, J. Organomet. Chem. 206 (1981) 77.
[36] D.J. Watkin, C.K. Prout, J.R. Carruthers, P.W. Betteridge, CRYSTALS (1996).
[37] D.J. Watkin, C.K. Prout, L.J. Pearce, CAMERON (1996).
[38] A. Altomare, G. Carascano, C. Giacovazzo, A. Guagliardi, J. Appl. Crystallogr. 26 (1993) 343.
[39] S.H. Vosko, L. Wilk, M. Nusair, Can. J. Phys. 58 (1990) 1200.
[40] A.D. Becke, Phys. Rev. A 38 (1988) 2398.
[41] J. Perdew, Phys. Rev. B 33 (1986) 8822.
[42] E.J. Baerends, E.G. Ellis, P. Ros, Chem. Phys. 2 (1973) 41.
[43] C. Fonseca Guerra, J.G. Snijider, B. te Velde, E.J. Baerends, Theor. Chem. Acc. 99 (1998) 391.
[44] B. te Velde, E.J. Baerends, J. Comput. Phys. 99 (1992) 84.
[45] L. Verluis, T. Ziegler, J. Chem. Phys. 88 (1988) 322.
[46] ADF2002.01, Theoretical Chemistry, Vrije Universiteit, Amsterdam, The Netherlands, http://www.scm.com.